

## Gasdynamics of Aerosol Deposition Method

H. Katanoda and K. Matsuo\*

Kagoshima University, 1-21-40 Koorimoto, Kagoshima, 890-0065 JAPAN

Fax: 81- 99-285-8250, e-mail: katanoda@mech.kagoshima-u.ac.jp

\* The University of Kitakyushu, 1-1 Hibikino, Wakamatsu-ku, Kitakyushu, Fukuoka, 808-0135 JAPAN

Fax: 81- 93-695-3394, e-mail: matsuo@env.kitakyu-u.ac.jp

The gas/particle flows of the aerosol deposition method are calculated by the method of computational fluid dynamics (CFD). Two-dimensional nozzles (sonic and supersonic) are used in the CFD model. The effects of the nozzle geometry and stagnation pressure upstream of the nozzle on both gas velocity and particle velocity are investigated. The computational results clarify that the larger particle velocity can be obtained by using a supersonic nozzle instead of using a sonic nozzle. This is because, the process gas is accelerated to a supersonic speed in the diverging part of the supersonic nozzle, causing the particle to reach a higher velocity.

Key words: aerosol deposition method, gasdynamics, supersonic jet, nozzle, numerical simulation

### 1. INTRODUCTION

The aerosol deposition method<sup>[1]</sup> (ADM) uses helium or nitrogen as a process gas at room temperature, and needs no additional heat energy to deposit ceramics particles on a substrate placed in a vacuum chamber.

The ADM seems to be an attractive technology in the field of the dry coating process. However, the mechanism of how ceramics particles deposit on a substrate has not been clarified yet. According to the experimental result, the impact velocity of particles onto the substrate is one of the important parameters to control coating properties.

Generally speaking, the stagnation pressure upstream of the nozzle is more than ten times the pressure in the vacuum chamber (back pressure) in ADM. In this case, the gas flow expands to back pressure through expansion waves originated at the lip of the nozzle exit. When the jet flow is supersonic just upstream of the substrate, the flow decelerates to subsonic speed through a shock wave. In the field of gasdynamics, which is the authors' interest, the gas flow of this type is called an under-expanded impinging jet. Such a kind of jet flow has been extensively studied in the past<sup>[2, 3]</sup>, however, mostly restricted to turbulent flow which can not be applied to laminar flow of ADM. Therefore, the gasdynamic research of ADM is essential for the understanding and the improvement of the process.

The present research investigates the gas flows of impinging jet of ADM as well as particle flow by using numerical simulation. The effects of nozzle geometry and stagnation pressure upstream of the nozzle on jet flows, and particle velocities are clarified.

### 2. NUMERICAL METHOD

#### 2.1 Gas flow

The flow is assumed to be two-dimensional in the computational fluid dynamics (CFD) model. The governing equations of the gas flow are given by the conservation form of the two-dimensional, time-dependent Navier-Stokes equations along with the equation of state. The flow is assumed to be laminar as

described later in this section. The governing equations are solved sequentially in an implicit, iterative manner using a finite difference formulation. For the present calculations, the governing equations are solved with the Chakravarthy-Osher type third-order, upwind, total variation diminishing scheme for the convective terms. A second-order, central difference scheme is used for the diffusive terms.

The working gas in the CFD model is nitrogen. The stagnation pressure upstream of the nozzle,  $p_{os}$ , was set at constant values ranging from 1 kPa to 10 kPa in CFD. The back pressure  $p_b$  was fixed at 100 Pa. The stagnation temperature of nitrogen gas both upstream of the nozzle and outside the nozzle was set at 300 K.

Figure 1 shows the geometry of two-dimensional nozzle used in the CFD model. Two types of nozzle configurations were tested; a sonic nozzle (a) and a supersonic nozzle (b). Both of them have a throat height of 0.4 mm, discharging the same mass flow rate at the same stagnation pressure  $p_{os}$ . The supersonic nozzle has an exit height of 1.2 mm.

The Reynolds number  $R_e$  calculated by the density, velocity, viscosity and a throat height is less than around

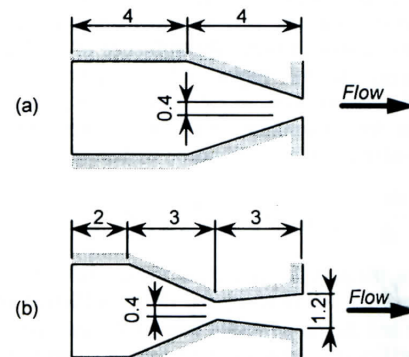


Fig.1 Simulated geometry of sonic nozzle (a) and supersonic nozzle (b) (unit : mm)

$10^3$  in the CFD. According to Troutt and McLaughlin<sup>[4]</sup> the jet flow is laminar for  $Re < 10^3$ . Therefore, the flow can be assumed to be laminar as stated before in this section.

The computational domain for the sonic nozzle is shown in Fig.2. The thick solid line shows the boundary of the computational domain. The nitrogen gas is discharged from the sonic nozzle towards the substrate. The distance from the nozzle exit to the substrate (stand-off distance) is 15 mm. The same computational domain between the nozzle exit to the substrate was also used for the supersonic nozzle.

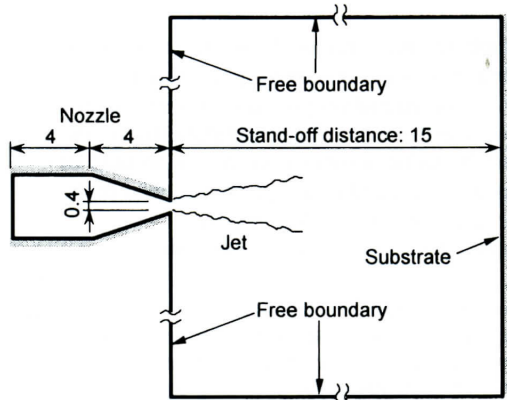


Fig.2 Computational domain for sonic nozzle (unit : mm)

## 2.2 Particle flow

To describe the particle motion, we use the Lagrangian formulation. The following assumptions are made to simplify the analysis.

- (1) The particles are spherical in shape.
- (2) The interaction between particles can be ignored.
- (3) The only force acting on a particle is drag force.
- (4) The presence of particles has a negligible effect on the gas velocity and temperature field.
- (5) The particles have a constant specific heat and a constant density.
- (6) The temperature in the particle is uniform.

As a result of the assumptions presented above, the gas-solid two-phase problem can then be independently solved. One can simulate the gas flow first, then use the resulting thermal and velocity fields to study the flow of different particles. The particle velocities were determined from a step-wise integration of their equations of motion under the influence of gasdynamic drag force. In this paper, only the particle motion along the center line is calculated. The governing equation for momentum transfer between a single particle of mass  $m_p$  and gas can be written as

$$m_p \frac{du_p}{dt} = \frac{1}{2} c_d \rho_g (u_g - u_p) |u_g - u_p| A_p \quad (1)$$

where,  $u_p$  the particle velocity,  $u_g$  the gas velocity,  $\rho_g$  the gas density,  $t$  the time,  $c_d$  the drag coefficient of the particle and  $A_p$  the projected area of the particle. The drag coefficient,  $c_d$ , was given by the equations proposed by Henderson<sup>[5]</sup>. The particle temperatures were also calculated by solving the unsteady heat-transfer equation of a sphere particle in a gas flow to calculate  $c_d$ . The

powder material used in the simulation is  $Pb(Zr,Ti)O_3$  (PZT) and the density is set as  $7,500 \text{ kg/m}^3$ .

## 3. RESULTS AND DISCUSSION

### 3.1 Code validation

To validate the two-phase flow model and numerical solution procedure, we selected the experimental data of Ref. [6] as the test case. The measured data includes velocities of PZT particle accelerated by nitrogen jet from a sonic nozzle with 0.4 mm exit-height. In Ref. [6], the particle velocity was measured by using a slitted cell which transverses the gas/particle flow to catch a flowing cloud of the particle. The detail of the method can be found in Ref. [1].

Figure 3 shows the comparison of the calculated and measured particle velocities. In the computation, the diameter of PZT particle was taken as  $0.2 \mu\text{m}$ <sup>[1]</sup>. Because the configuration of the sonic nozzle is not described in Ref. [6] other than the exit-height of 0.4 mm, the nozzle configuration of Fig.1(a) was used for the test case. The detail of the computational method is described in Ref. [8]. As can be seen in Fig.3, the computational and experimental results compare well.

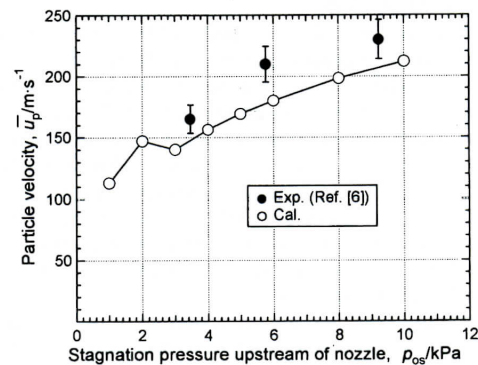


Fig.3 Comparison of particle velocity

### 3.2 Gas flow

Figure 4 shows simulated Mach number contour of the gas flow at the stagnation pressure  $p_{os} = 2 \text{ kPa}$  for the sonic nozzle (a) and the supersonic nozzle (b). For the sonic nozzle, Fig.4(a), the static pressure at nozzle exit is larger than the back pressure. Therefore, the gas expands into the vacuum chamber through expansion waves originated at the nozzle lip. The cell structure of the jet is called shock-cell. Two shock-cells are visible in Fig.4(a) and the gas flow reaches maximum Mach number of 3.3 in the first shock-cell. The extent of expansion of the gas flow is not so large as to form a shock wave on the center line.

For the supersonic nozzle, Fig.4(b), the extent of expansion of the jet is smaller than that for Fig.4(a). This is because the gas flow has further expanded than the sonic nozzle through the diverging part to accelerate to supersonic velocity. Then, the static pressure at the exit of the supersonic nozzle is smaller compared to the sonic nozzle. As a result, the extent of expansion in the jet becomes smaller for the supersonic nozzle compared to the sonic nozzle. The maximum Mach number is 2.4 in the first shock-cell in Fig.4(b).

Figure 5 shows simulated Mach number contour of

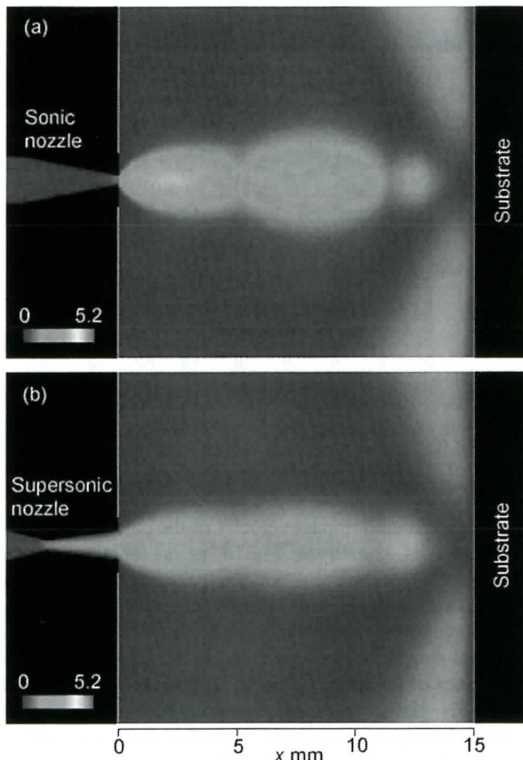


Fig.4 Mach number contours at  $p_{os} = 2$  kPa for sonic nozzle (a) and supersonic nozzle (b)

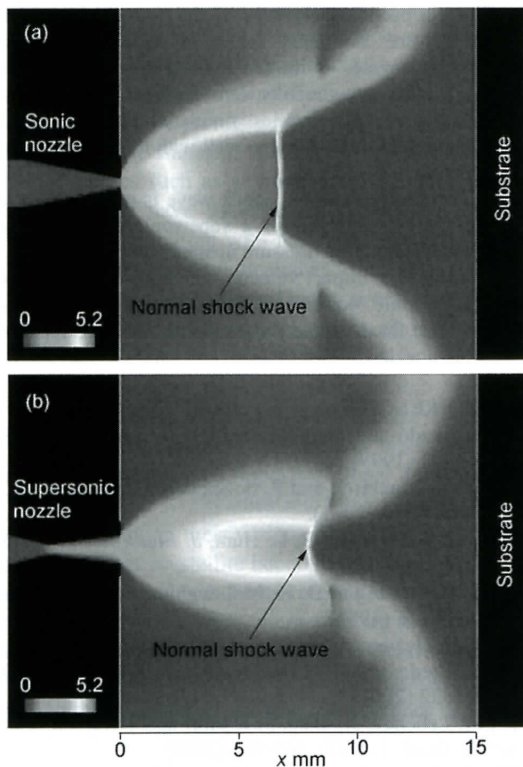


Fig.5 Mach number contours at  $p_{os} = 6$  kPa for sonic nozzle (a) and supersonic nozzle (b)

the gas flow at the stagnation pressure  $p_{os} = 6$  kPa for the sonic nozzle (a) and the supersonic nozzle (b). For the sonic nozzle, Fig.5(a), the gas is strongly expanded into the vacuum chamber compared to the same nozzle of Fig.4(a). This is because, the static pressure at the nozzle exit of Fig.5(a) is three times larger than that of Fig.4(a). The larger the extent of the gas expansion becomes, the larger the spreading angle of the jet becomes at the nozzle exit. The expansion is so strong that a shock wave which is perpendicular to the flow direction is generated at  $x = 7$  mm in Fig.5(a). It is called a normal shock wave in the field of gasdynamics. The Mach number reaches the maximum value of 5.2 just upstream of the normal shock wave. The larger Mach number causes the stronger normal shock wave.

For the supersonic nozzle, Fig.5(b), the extent of the gas expansion at the nozzle exit, that is the spreading angle of the jet, is smaller than that of Fig.5(a). This is due to the smaller static pressure at the supersonic nozzle exit compared to that of the sonic nozzle exit, resulting in a smaller extent of expansion.

Calculated gas velocity along the center line for the sonic nozzle is shown in Fig.6. The gas velocity repeats acceleration and deceleration outside the nozzle due to the shock-cell structure for  $p_{os} = 2$  kPa. For  $p_{os}$  larger than or equal to 6 kPa, the gas velocity shows an abrupt drop by going through the normal shock wave. The location of the normal shock wave goes downstream as  $p_{os}$  is increased.

Calculated gas velocity along the center line for the supersonic nozzle is shown in Fig.7. The normal shock wave is also generated in this case for  $p_{os}$  larger than or

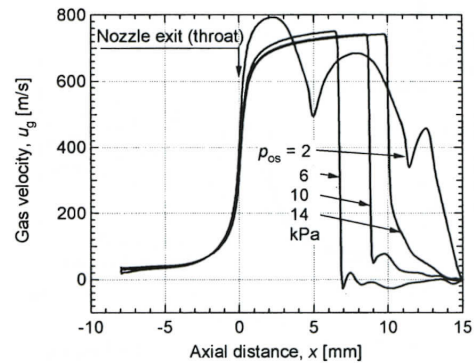


Fig.6 Gas velocity along center line for sonic nozzle

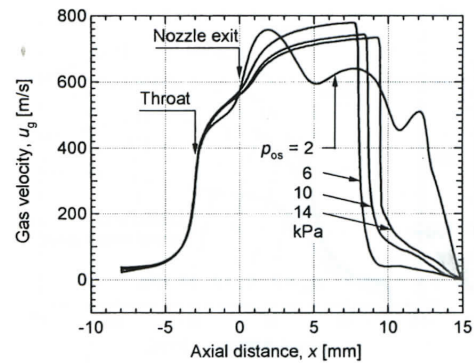


Fig.7 Gas velocity along center line for supersonic nozzle

equal to 6 kPa. The location of the normal shock wave, however, is less affected by increasing  $p_{os}$  compared to the sonic nozzle (Fig.6). The onset of generation of the normal shock wave is at  $p_{os}$  smaller than 6 kPa for the two nozzles as shown later in Fig.10.

### 3.3 Particle velocity

Calculated particle velocity along the center line for the sonic nozzle is shown in Fig.8. After a large amount of acceleration at the nozzle exit, the particle continues acceleration towards the substrate through the jet stream with no shock wave for  $p_{os} = 2$  kPa. For  $p_{os} \geq 6$  kPa, the larger  $p_{os}$  results in larger particle velocity along the center line. However, the particle velocity decreases after passing through the normal shock wave. This is because, the particle velocity is larger than the gas velocity between the normal shock wave and the substrate.

Calculated gas velocity along the center line for the supersonic nozzle is shown in Fig.9. As for  $p_{os} = 2$  kPa, the impact velocity of the particle is around 30 m/s larger than that for the sonic nozzle. This is because, the particle continues acceleration through the diverging part of the nozzle. Then, the particle reaches higher velocity at the supersonic nozzle exit than at the sonic nozzle exit. Because of the same reason, the particle impact velocity of the supersonic nozzle is larger than that of the sonic nozzle for every value of  $p_{os}$  in this simulation. The extent of acceleration of the particle in the jet flow is not so different for the two nozzles.

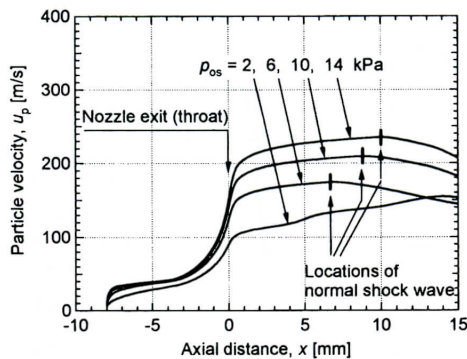


Fig.8 Particle velocity along center line for sonic nozzle

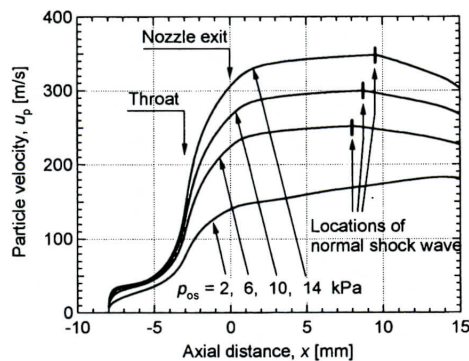


Fig.9 Gas velocity along center line for supersonic nozzle

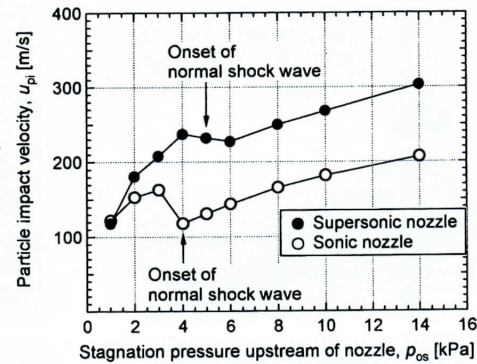


Fig.10 Particle impact velocity versus stagnation pressure upstream of nozzle

The simulated impact velocity of the particle onto the substrate is shown in Fig.10 as a function of the stagnation pressure  $p_{os}$  for the two nozzles. For the sonic nozzle, the impact velocity increases by increasing the stagnation pressure  $p_{os}$  except for 4 kPa where the normal shock wave is generated in the jet. The overall tendency of the impact velocity is true for the supersonic nozzle. The most remarkable point in Fig.10 is that by using the supersonic nozzle the higher impact velocity is obtained compared to using the sonic nozzle for the same stagnation pressure  $p_{os}$ .

### 4. CONCLUSIONS

The gas/particle velocities of the aerosol deposition method were simulated for a sonic nozzle and a supersonic nozzle. Nitrogen gas was used as a process gas. The following results were obtained;

- (1) The particle velocities simulated by the present numerical method agree well with the experimental results.
- (2) The stronger normal shock wave is generated for a sonic nozzle than for a supersonic nozzle at the same stagnation pressure upstream of the nozzle.
- (3) The larger impact velocity is obtained by using the supersonic nozzle compared to using the sonic nozzle for the same stagnation pressure upstream of the nozzle.

### 5. REFERENCES

- [1] J. Akedo and M. Lebedev: *Jpn. J. Appl. Phys.*, 33, 5397-5401 (1999).
- [2] C. D. Donaldson and R. S. Snedeker, *J. Fluid Mech.*, 45(2), 281-319 (1971).
- [3] J. C. Carling and B. L. Hunt, *J. Fluid Mech.*, 66(1), 159-176 (1974).
- [4] T. R. Troutt and D. K. McLaughlin, *J. Fluid Mech.*, 116, 123-156 (1982).
- [5] C. B. Henderson, *AIAA J.*, 14(6), 707-708 (1976).
- [6] J. Akedo and M. Lebedev, *Jpn. J. Appl. Phys.*, 40, 5528-5532 (2001).
- [7] M. Lebedev, J. Akedo, M. Mori and T. Eiju, *J. Vac. Sci. Technol. A*, 18(2), 563-566 (2000).
- [8] H. Katanoda and K. Matsuo, *Proc. 1st ATSC*, Nagoya, 17-18 (2005).

(Received December 10, 2005; Accepted September 30, 2006)